

RSC Advances



This is an *Accepted Manuscript*, which has been through the Royal Society of Chemistry peer review process and has been accepted for publication.

Accepted Manuscripts are published online shortly after acceptance, before technical editing, formatting and proof reading. Using this free service, authors can make their results available to the community, in citable form, before we publish the edited article. This *Accepted Manuscript* will be replaced by the edited, formatted and paginated article as soon as this is available.

You can find more information about *Accepted Manuscripts* in the [Information for Authors](#).

Please note that technical editing may introduce minor changes to the text and/or graphics, which may alter content. The journal's standard [Terms & Conditions](#) and the [Ethical guidelines](#) still apply. In no event shall the Royal Society of Chemistry be held responsible for any errors or omissions in this *Accepted Manuscript* or any consequences arising from the use of any information it contains.

Microstructures, mechanical and tribological properties of VN films deposited by PLD technique

Hongjian Guo,^{a,b,c} Bo Li,^a Jianyi Wang,^{a,b} Wenyuan Chen,^{a,b} Zhenyu Zhang,^c

Wenzhen Wang,^a Junhong Jia^{a*},

^a State Key Laboratory of Solid Lubrication, Lanzhou Institute of Chemical Physics, Chinese Academy of Sciences, Lanzhou 730000, China,

^b Graduate University of Chinese Academy of Sciences, Beijing 100049, China,

^c Lanzhou Institute of Technology, Lanzhou 730000, China,

Abstract

The consistent stoichiometric fcc structure VN films were fabricated by pulsed laser deposition (PLD) technique at room temperature and 300 °C, for which the microstructures, mechanical and tribological properties were investigated systematically. The results indicated that the films deposited at 300 °C displayed a denser structure, and possessed higher hardness and elastic modulus values than the films deposited at room temperature which exhibited a columnar structure. The wear behaviors of VN films were investigated at elevated temperature to 900 °C against alumina ball in ambient atmosphere. Due to the densification structure and excellent mechanical properties, the VN films deposited at 300 °C held lower friction coefficient over the investigated temperature range compared to the films deposited at room temperature, and registered the lowest friction coefficient about 0.21 at temperature of 900 °C. According to the XRD and Raman spectroscopy results, the oxidation behaviors of VN films at elevated temperatures formed a series of vanadium oxides, such as V₂O₅, V₃O₇, V₆O₁₁, V₆O₁₃ and so on, which displayed easy

* Corresponding author. J. Jia. Tel: +86 931 4968611. Fax: +86 931 8277088. E-mail: jhjjia@licp.cas.cn.

crystallographic shear planes with reduced binding strength and influenced the tribological properties significantly. Moreover, the liquid self-lubrication existed in the tribology process above 700 °C due to the melting of V_2O_5 which registered low melting points of 680 °C. Combining vanadium oxides phase as lubrication phases with lubricious oxide layer, and as well as the liquid lubrication in the contact area, can be reasonable for the decreased friction coefficients at higher temperatures.

Keywords: VN film; Pulsed laser deposition; Microstructure; Tribological property; vanadium oxides

1. Introduction

Transition metal nitrides, i.e., titanium nitride (TiN) and vanadium nitride (VN) have attracted great attention over the past decades due to their excellent physical and chemical properties, including high melting point, metal-like conductivity, good chemical stability, and high hardness¹⁻⁷. Moreover, the TiN and VN have been widely used in various researches such as: optical devices^{8,9}, microelectronics^{10,11}, catalyse^{12,13}, energy storage devices¹⁴⁻¹⁶ like batteries and supercapacitors, tribological utilisation¹⁷⁻¹⁹. In particular, the vanadium nitride in the form of thin films have been focused in high-temperature protective and lubrication applications for decade years^{2,7, 18-24}, which not only enhanced the properties of common films, but also formed lubricious vanadium oxides on the wear track during friction process at elevated temperatures, often referred to as Magnéli phases. As a matter of fact, a variety of vanadium oxides represent oxygen deficient homologous series with planar faults, show easy crystallographic shear planes with reduced binding strength, which can

play a lubrication role in high-temperature friction^{2, 7, 20, 23}. In addition, the liquid self-lubrication often exist in tribo-contact area due to that these formed oxide phases usually show low melting points, such as V_2O_5 with melting point of 680 °C will be in the form of liquid at the temperature above 700 °C²⁵. Therefore, the vanadium nitride is supposed to be an effective candidate for high-temperature lubrication materials.

In recent years, several techniques have been utilized to deposit VN thin films, such as chemical vapour deposition¹⁴, ion plate¹⁸ and magnetron sputtering^{11, 20, 21, 23, 25}, but the VN films prepared by pulsed laser deposition (PLD) technique and used in high-temperature lubrication are really rare. The PLD technique is more advantageous than the other methods due to its high deposition rate and good uniformity. Furthermore, the tribological properties and oxidation of VN films were characterized at elevated temperatures only to 700 °C in early literatures,^{18, 20, 21} while in present work, the VN films deposited by PLD technique, for which microstructures and mechanical properties were investigated in detail, but also tribological behavior was evaluated from room temperature to 900 °C in ambient atmosphere. It is expected that the prepared VN films with satisfied mechanical and tribological properties could be a potential application in high-temperature lubrication.

2. Experimental details

2.1. Films preparation

The VN films were deposited on silicon wafer and Inconel 718 substrates by PLD technique using a KrF excimer laser ($\lambda = 248$ nm, pulse duration = 25 ns, ComPexPro 205) at room temperature and 300 °C, and then the samples were denoted as VN_{RT},

VN₃₀₀, respectively. The individual VN target with a dimension of $\Phi 60$ mm \times 5 mm and 99.99% purity was used as source material. The details of the deposition process have been reported elsewhere²⁶. Briefly, a VN target was irradiated with 300 mJ of pulsed laser energy at 10 Hz in 36000 pulses for each sample, the target was placed parallel to substrate at a distance of approximately 50 mm. Prior to ablating the target, the deposition system was evacuated to 6.0×10^{-5} Pa and the working gas pressure was set to 0.3 Pa by the N₂ flow of 90 ml/min.

2.2. Films characterization

The X-ray diffraction (Philips, Cu K α radiation, $\lambda=0.15$ nm) technique was conducted to investigate the phase composition and identify possible oxide phases formed after tribological test by comparing to standard ICSD patterns (89/54378) data files with Jade6.0 software. The measurement was running at a potential of 40 kV and current of 40 mA, the scanning range of 2θ was from 15° to 80° at the grazing incidence angle of 1°, the scan step size was fixed at 0.06 °/s. The crystallite size of the films was calculated by the Scherrer equation and Williamson–Hall plot method²⁷. The microstructure morphologies of the films were characterized by SU-8020 scanning electron microscope. The micro-hardness and elastic modulus of the films were evaluated using insitu nanomechanical testing system (TI950, Hysitron TriboIndenter, USA) with a cube-corner diamond tip and set to run five indents on each sample.

The tribological behavior of the VN films was conducted by a ball-on-disk tribometer (UMT-3, Bruker) at elevated temperatures from room temperature up to

900 °C against alumina ball (10mm in diameter) in ambient atmosphere (relative humidity of $40\pm 5\%$). The rotated tests run at the rotated velocity of 200 rpm with the radius of 3 mm under the normal load of 10N in 10 min for every sample. The tribochemical reactions and wear products during the rotated tests were monitored by Raman spectroscopy (Horiba Raman microscope, He-Ne laser, wave length of 532 nm).

3. Results and discussion

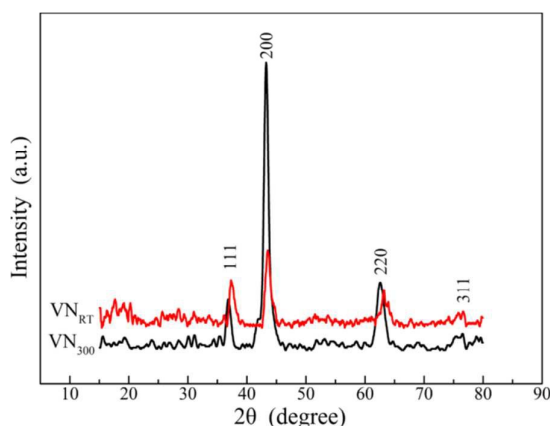


Fig.1 GIXRD patterns of the VN_{RT} and VN₃₀₀ films

3.1. Microstructures

Fig. 1 shows the grazing incidence X-ray diffraction (GIXRD) patterns of VN films deposited at room temperature and 300 °C, indicating that the consistent stoichiometric vanadium nitride films exhibit polycrystalline fcc VN structure^{20,21}. In the case of the VN_{RT} film, there is no obvious difference in peak intensity but still with a light texture at the [200] direction because it presents the highest intensity. As the substrate temperature increasing, the VN₃₀₀ film strongly oriented in [200] orientation, suggesting that it retains the largest volume fraction in the film. The preferred orientation observed in the films as a function of the deposition temperatures have been explained detailly in our previous work²⁶, where the TiN

films showed a strong [200] orientation at higher temperatures can be explained by considering the competition between surface energy and epitaxy. The Lattice parameter, Grain size and Micro-strain were calculated on the basis of the patterns in Fig. 1 and tabulated in Table 1. There is no significant change in the lattice parameters of the deposited films at different substrate temperatures. While the VN films possess small grain size in the range of 8-10 nm can be due to the formation of highly textured grains and the texture-controlled grain growth in addition to the higher nucleation kinetics during the deposition, as reported in Jayaganthan's work²⁸ that the formation of nanograins in the TiN films influenced by factors such as ion energy, ion flux, trace impurities, and textures. In addition, all peaks of the VN₃₀₀ film shift to lower diffraction angles than the value of VN_{RT} which may be due to the influence of the enhanced surface energy and mobility of adatoms at higher substrate temperature and the residual compressive stresses^{20, 29}, and results in higher Micro-strain of the VN₃₀₀ film.

Table 1 Structural parameters of the VN_{RT} and VN₃₀₀ films

Samples	Lattice parameter /nm	Grain size/nm	Micro-strain /%
VN _{RT}	0.4113	8.2(0.2)	0.907(0.11)
VN ₃₀₀	0.4116	9.7(0.3)	0.549(0.08)

The surface and section morphology of the VN_{RT} and VN₃₀₀ films are shown in Fig.2. It can be seen clearly that the surface of VN_{RT} film is much coarser and looser than that of VN₃₀₀ film. There are some large cauliflower-like particles about 400-600 nm in diameter on the VN_{RT} film surface. On the contrary, the VN₃₀₀ film surface is very flat and compact, and nearly had no larger particles except some ball-like with a

diameter of 100 nm on the surface. There is also an evident difference in section morphology between the VN_{RT} and the VN_{300} films, the former with the thickness of 1.2 μm display a typical columnar structure but the latter with 1.4 μm show a densification structure. The growth rate and the crystallization are enhanced at higher deposition temperatures compared to room temperature due to that the PLD films growth depended on the mobility of ad-atoms and their diffusion. At room temperature, the adatoms with high temperature and energy arrived on the pre-deposited surface, the film grows along the opposite direction of heat-transfer, and results in a typical columnar structure. At higher substrate temperature for the VN_{300} film, the high-energy-mobility adatoms move along the random directions on the pre-deposited surface, meet and aggregate together, and results in enhancing the crystallization and formation of a dense microstructure. This phenomenon is similar to a dense structure TiN film fabricated by unbalanced D.C. magnetron sputtering³⁰, also agree well with the early investigations that the VN¹⁰ and TiN²⁶ films obtained at higher temperature was thicker than the films deposited at room temperature.

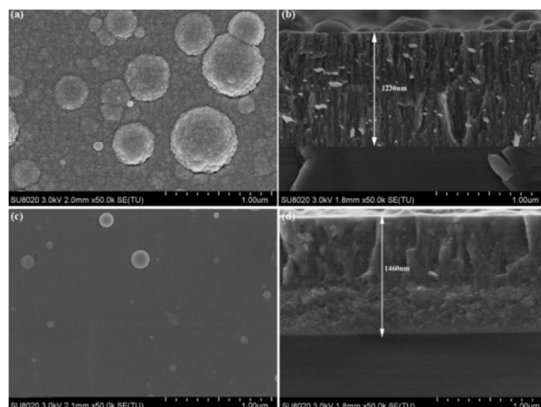


Fig. 2 SEM images of the VN films (a,b) VN_{RT} , (c,d) VN_{300}

3.2. Mechanical properties

The results of nanoindentation measurements on VN films deposited at different temperatures are presented in Fig. 3. It is obvious that the hardness and elastic modulus of VN_{RT} films are lower than that of VN₃₀₀ films which hold the maximum hardness and elastic modulus value of 21.5 GPa, 256.8 GPa respectively. To exclude the influence of substrates, the nanoindentation experiments were performed in the controlled contact depth of 60, 120 and 200 nm. Take the VN₃₀₀ films for example as insert in Fig. 3, there is small difference among the results, especially in the controlled contact depth of 200nm where the five load-displacement curves are in coincidence basically. It is worth mentioning that the mechanical properties of the VN₃₀₀ films are uniformly. The results of VN films are higher than that of the magnetron sputtering VN films¹¹ where the hardness and elastic modulus are 11 GPa and 187 GPa, respectively. The mechanical properties of the films have a direct correspondence relationship to microstructures. There was also a wealth of information available in early studies³¹ that the deformation mechanisms are different at the different grain sizes of the materials. When the grain size was in the range of 1-20 nm, grain-boundary sliding became important and had been identified that grain-boundary effects dominated the deformation process. As analysed by microstructure results, both of the prepared VN films exhibited nanograins in the size of 8-10 nm, when exerted an external load on the films, where the sliding occurred at every grain boundary and dislocation density increased due to the most grain boundaries, and could resist the external load validly. However, the columnar structure such as the VN_{RT} film contains more intergranular cracking during indentation tests than that of

the VN₃₀₀ films which display a dense and flat structure^{32,33}. Consequently, a denser microstructure, small grain size and higher residual compressive stress may be an important contribution to the higher hardness and elastic modulus of the VN₃₀₀ films^{34,35}.

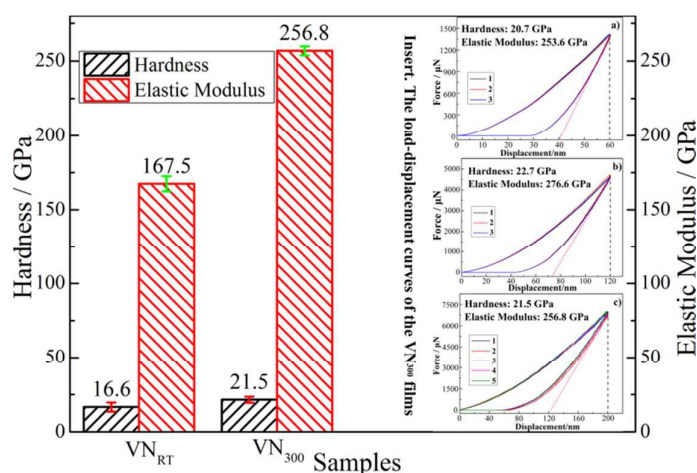


Fig. 3 The hardness and elastic modulus of the VN_{RT} and VN₃₀₀ films
Insert: the load-displacement curves of VN₃₀₀ films (a-60nm, b-120nm, c-200nm)

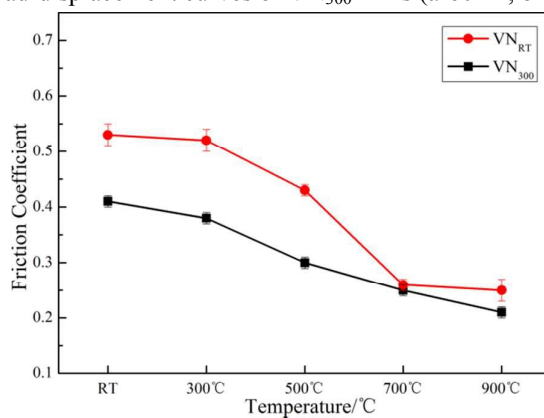


Fig. 4 Temperature dependence of friction coefficient for the VN_{RT} and VN₃₀₀ films

The stationary friction coefficients as a function of temperatures for the VN_{RT} and VN₃₀₀ films are shown in Fig. 4. Obviously, the VN₃₀₀ films show lower friction coefficients over the whole test temperature range compared with the VN_{RT} films. At lower temperatures, both the VN films display a little difference in friction coefficients respectively. However, the films exhibit decreased friction coefficients at

higher temperatures, and both of that drop to a similar level at higher temperatures around 700 °C (VN_{RT} -0.26, VN_{300} -0.25). While it may be due to continuous formation of easy-sheared vanadium oxide phases and lubricious layer in the tribo-contact area^{21, 25, 34}. According to previous statement^{2, 7, 20, 23}, a variety of vanadium oxides formed on worn surface display a low shear strength due to its crystallographic structure, which can play a significant lubrication role in the contact area during high-temperature friction. Additionally, the liquid self-lubrication often exists in the contact area due to melting of V_2O_5 (with melting point~680 °C) above 700 °C, which could be contributed to the similar friction coefficients at 700 °C for both films. Therefore, vanadium oxides and protective lubricious oxide layer formed in the wear track during tests, as well as the liquid lubrication in the contact area, can be reasonable for the VN films possess a decreased friction coefficient at higher temperatures. Furthermore, increased hardness is also reported to lead to better wear resistance³⁵, the denser microstructure combined with excellent mechanical properties of the VN_{300} film may be consequently responsible for better tribological property compare to the VN_{RT} film. In addition, it was found that the friction coefficients were slightly lower than that of VN films (μ ~0.45-0.25) prepared by reactive unbalanced magnetron sputtering in early studies^{20, 23}, where the wear tests were performed from room temperature to 700 °C against alumina ceramic ball (6mm in diameter) at a load of 5 N in the humid air.

In order to illustrate the tribology process of the films at different temperatures, the friction coefficients curves corresponding to test time for VN_{300} films are shown in

Fig. 5, which are mainly steady during the friction tests. After a very short running-in period, the friction coefficient slightly decreases and reaches a steady condition. In combination with the homogeneous dense microstructure and excellent mechanical properties, could be reasonably contributed to the steady friction process of the VN₃₀₀ films. It might also be concluded that the films deposited by PLD technique at 300 °C were greatly uniform.

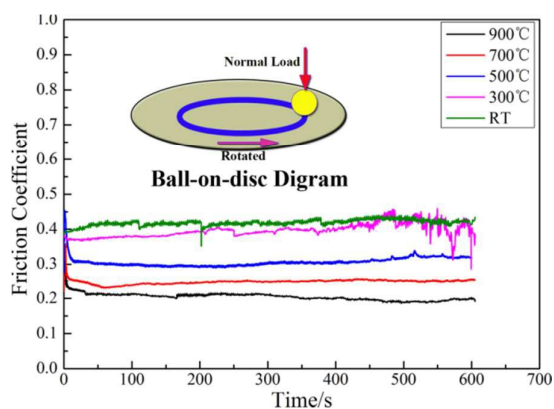


Fig. 5 The friction vs rotated time curves of the VN₃₀₀ film at different temperatures

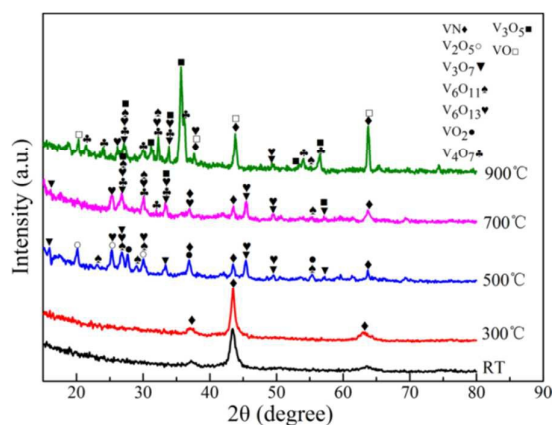


Fig. 6 GIXRD patterns of the VN₃₀₀ film after tribological test at different temperatures

In order to explain the phenomenon that the friction coefficients decreased with the temperatures increasing, the films after tribological tests are characterized using GIXRD analysis for oxide phases identification. Take the VN₃₀₀ film for example, as

shown in Fig. 6. It can be apparently seen that an fcc VN structure is stable from room temperature to 300 °C, and there is no significant oxidation can be observed until test temperature up to 500 °C. A high quantities of new peaks in the XRD pattern indicating generation of various vanadium oxides on the film surface at 500 °C, which can be intended to be V₂O₅, VO₂, V₃O₇, V₆O₁₁, V₆O₁₃. As the test temperatures rises to 700 and 900 °C, more vanadium oxides can be identified as V₃O₇, V₃O₅, V₄O₇, V₆O₁₁, V₆O₁₃. Furthermore, since only a very weak signal of the VN peaks can be observed at higher temperatures, suggesting that a massive oxidation took place on the film surface. For many materials, there is a transformation temperature at which a continuous oxidation occurred and oxide layer established, which give good protection against wear^{2, 23, 36, 37}. For the VN, oxidation starts to take place above the temperature of 400 °C, the formed vanadium oxides also undergo a reversible change in the crystal structure during the wear test at its transformation temperature^{38, 39}, leading to phase transformations such as V₂O₅ which predominates in the XRD patterns of the oxidized VN films surface at 500 °C but disappear at higher temperatures, and new V₄O₇, V₃O₅ phase appears in the XRD patterns. On the basis of other reports^{20, 21, 23}, the vanadium oxides can be assigned to the lubricious Magnéli oxide series V_nO_{2n-1} and V_nO_{3n-1} with n=1, 2, 3, which exhibited easy crystallographic shear planar with reduced binding strength, and played a significant lubrication role in the contact area during high-temperature friction, and results in a decreased friction coefficient with the temperature increasing.

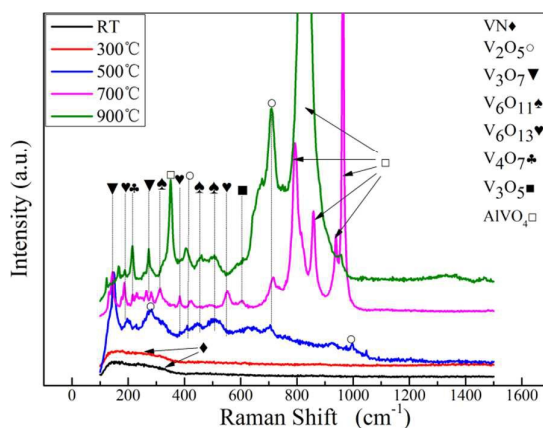


Fig. 7 Raman patterns of wear track on the VN₃₀₀ film after tribological test at different temperatures

For a further investigation of oxidation products, the wear track of VN₃₀₀ films after test at different temperatures have been analysed by Raman spectroscopy, as shown in Fig. 7. Raman investigations indicate that the patterns obtained at room temperature and 300 °C show the standard curves of stoichiometry VN, which agree well with the reports in Refs^{20, 23}. As the test temperature increasing to 500 °C, the significant peaks suggesting the ongoing oxidation reactions during the tribological test which can be identified as V₂O₅, V₃O₇, V₆O₁₁, V₆O₁₃, the results mainly agree to above XRD results. In the case of wear track produced at 700 and 900 °C, apart from the vanadium oxides that the XRD investigations have detected, a high amount of new phase corresponding to AlVO₄ can be observed, which exist in the range between 900 and 1000 cm⁻¹. The generation of AlVO₄ is assumed to be an interaction between the formed V₂O₅ and the alumina counterpart during the high-temperature tribological test²⁰. Combining with lubrication action of vanadium oxides and AlVO₄ phase are supposed to be reasonable for the low friction coefficients for both types of films. Furthermore, the AlVO₄ peaks predominate in both Raman patterns but not tested by XRD investigation, it may result from that Raman spectroscopy investigate the tiny area on wear track, but XRD

investigation conducted in larger area consist of both wear track and surface of the films.

4. Conclusions

The aim of this work was to investigate the microstructures, mechanical and tribological properties of the VN films which were fabricated by PLD technique. Results from these studies revealed that:

- (1) The VN film deposited at 300 °C displayed a densification structure, and possessed higher hardness and elastic modulus values than the film deposited at room temperature which registered looser columnar structure.
- (2) The VN films exhibited decreased friction coefficients at higher temperatures, which deposited at 300 °C held lower friction coefficient over the investigated temperature range compared to the films deposited at room temperature due to its densification structure and excellent mechanical properties, and registered the lowest friction coefficient about 0.21 at the temperature of 900 °C.
- (3) The oxidation behavior of VN films at elevated temperatures formed a series of vanadium oxides which influenced the tribological properties. In combination with lubricious oxidation products (vanadium oxides) and lubricious oxide layer, as well as the liquid lubrication in the contact area, could be responsible for the decreased friction coefficients at higher temperatures.

Acknowledgments

The authors gratefully acknowledge the National Natural Science Foundation of China (Grant No. 51471181), National Defense Science and Technology Innovation

Foundation of Chinese Academy of Sciences (Grant No. CXJJ-14-M39), the Young Science and Technology Foundation of Gansu Province (Grant No. 1506RJYA058), and the Project of Gansu Province Longyuan young Creative Talents (Grant No. 2015GS06462) in China for providing the financial support.

References

1. T. Fu, X. Peng, Y. Zhao, R. Sun, D. Yin, N. Hu and Z. Wang, *RSC Adv.*, 2015, 5, 77831-77838.
2. R. Franz and C. Mitterer, *Surface and Coatings Technology*, 2013, 228, 1-13.
3. O. Jantschner, C. Walter, C. Muratore, A. A. Voevodin and C. Mitterer, *Surface and Coatings Technology*, 2013, 228, 76-83.
4. G. J. W. N. Huang, Y. Leng, Y.X. Leng, H. Sun, P. Yang, J.Y. Chen, J. Wang, P.K. Chu, *Surface and Coatings Technology*, 2002, 156, 170-175.
5. S. Kataria, S. K. Srivastava, P. Kumar, G. Srinivas, Siju, J. Khan, D. V. S. Rao and H. C. Barshilia, *Surface and Coatings Technology*, 2012, 206, 4279-4286.
6. D. Craciun, N. Stefan, G. Socol, G. Dorcioman, E. McCumiskey, M. Hanna, C. R. Taylor, G. Bourne, E. Lambers, K. Siebein and V. Craciun, *Applied Surface Science*, 2012, 260, 2-6.
7. N. Fateh, G. A. Fontalvo and C. Mitterer, *Tribology Letters*, 2008, 30, 21-26.
8. Y. Xu, J. Wang, L. Shen, H. Dou and X. Zhang, *Electrochimica Acta*, 2015, 173, 680-686.
9. N. Fechler, G. A. Tiruye, R. Marcilla and M. Antonietti, *RSC Advances*, 2014, 4, 26981.
10. C. M. Ghimbeu, F. Sima, R. V. Ostaci, G. Socol, I. N. Mihailescu and C. Vix-Guterl, *Surface and Coatings Technology*, 2012, 211, 158-162.
11. J. C. Caicedo, G. Zambrano, W. Aperador, L. Escobar-Alarcon and E. Camps, *Applied Surface Science*, 2011, 258, 312-320.
12. T. Huang, J. Yu, J. Han, Z. Zhang, Y. Xing, C. Wen, X. Wu and Y. Zhang, *Journal of Power Sources*, 2015, 300, 483-490.
13. S. H. Taylor and A. J. J. Pollard, *Catalysis Today*, 2003, 81, 179-188.
14. I. P. Parkin and G. S. Elwin, *Journal of Materials Chemistry*, 2001, 11, 3120-3124.
15. T. C. M. Corbiere, D. Ressnig, C. Giordano and M. Antonietti, *RSC Advances*, 2013, 3, 15337.
16. C. Yang, H. Wang, S. Lu, C. Wu, Y. Liu, Q. Tan, D. Liang and Y. Xiang, *Electrochimica Acta*, 2015, 182, 834-840.
17. S. Oktay, Z. Kahraman, M. Urgan and K. Kazmanli, *Applied Surface Science*, 2015, 328, 255-261.
18. J. H. Ouyang, T. Murakami and S. Sasaki, *Wear*, 2007, 263, 1347-1353.
19. U. Wiklund, B. Casas and N. Stavlid, *Wear*, 2006, 261, 2-8.
20. N. Fateh, G. A. Fontalvo, G. Gassner and C. Mitterer, *Wear*, 2007, 262, 1152-1158.
21. K. Kutschej, P. H. Mayrhofer, M. Kathrein, P. Polcik and C. Mitterer, *Surface and Coatings Technology*, 2005, 200, 1731-1737.
22. W. Tillmann, S. Momeni and F. Hoffmann, *Tribology International*, 2013, 66, 324-329.
23. N. Fateh, G. A. Fontalvo, G. Gassner and C. Mitterer, *Tribology Letters*, 2007, 28, 1-7.
24. S. M. Aouadi, D. P. Singh, D. S. Stone, K. Polychronopoulou, F. Nahif, C. Rebholz, C. Muratore

- and A. A. Voevodin, *Acta Materialia*, 2010, 58, 5326-5331.
25. P. H. M. G. Gassner, K. Kutschej, C. Mitterer, M. Kathrein, *Tribology Letters*, 2004, 17, 751-756.
 26. H. Guo, W. Chen, Y. Shan, W. Wang, Z. Zhang and J. Jia, *Applied Surface Science*, 2015, 357, 473-478.
 27. D. Craciun, G. Socol, N. Stefan, G. Dorcioman, M. Hanna, C. R. Taylor, E. Lambers and V. Craciun, *Applied Surface Science*, 2014, 302, 124-128.
 28. V. Chawla, R. Jayaganthan and R. Chandra, *Materials Characterization*, 2008, 59, 1015-1020.
 29. C. P. Constable, D. B. Lewis, J. Yarwood and W. D. Münz, *Surface and Coatings Technology*, 2004, 184, 291-297.
 30. F. K. P.H. Mayrhofer, J. Musil, C. Mitterer, *Thin Solid Films*, 2002, 415, 151-159.
 31. M. A. Meyers, A. Mishra and D. J. Benson, *Progress in Materials Science*, 2006, 51, 427-556.
 32. F. Ge, P. Zhu, H. Wang, F. Meng, S. Li and F. Huang, *Wear*, 2014, 315, 17-24.
 33. J. M. Cairney, M. J. Hoffman, P. R. Munroe, P. J. Martin and A. Bendavid, *Thin Solid Films*, 2005, 479, 193-200.
 34. M. Pfeiler-Deutschmann, P. H. Mayrhofer, K. Chladil, M. Penoy, C. Michotte, M. Kathrein and C. Mitterer, *Thin Solid Films*, 2015, 581, 20-24.
 35. M. Pfeiler, K. Kutschej, M. Penoy, C. Michotte, C. Mitterer and M. Kathrein, *International Journal of Refractory Metals and Hard Materials*, 2009, 27, 502-506.
 36. P. H. Mayrhofer, C. Mitterer and J. Musil, *Surface and Coatings Technology*, 2003, 174-175, 725-731.
 37. S. M. Aouadi, B. Luster, P. Kohli, C. Muratore and A. A. Voevodin, *Surface and Coatings Technology*, 2009, 204, 962-968.
 38. O. K. E. Lugscheider, K. Bobzin, S. Barwulf, *Surface and Coatings Technology*, 2000, 133-134, 362-368.
 39. D. Porwal, A. C. M. Esther, I. N. Reddy, N. Sridhara, N. P. Yadav, D. Rangappa, P. Bera, C. Anandan, A. K. Sharma and A. Dey, *RSC Adv.*, 2015, 5, 35737-35745.